Multidisciplinary Characterization of Abundant Ferromanganese Microparticles in Deep-Sea Oxic Sediments: Implications for the Global Manganese Budget

Abundant (10^8–10^9 particles cm^{-3}) micrometer-scale ferromanganese mineral particles (Mn-microparticles) were found in deep-sea oxic sediments of the South Pacific Gyre from the seafloor to the ~100 million-year-old sediments. Microtexture, major and trace element composition, and synchrotron-based redox state analyses revealed that these Mn-microparticles consist of poorly crystalline ferromanganese oxides precipitating from bottom water. We extrapolate that 1.5–8.8 × 10^{28} Mn-microparticles, accounting for 1.28–7.62 Tt of manganese, are present globally. This estimate is at least two orders of magnitude larger than the manganese budget of manganese nodules and crusts on the seafloor. Thus, Mn-microparticles contribute significantly to the global manganese budget.

Manganese is the third most abundant metallic element, after iron and titanium, in the Earth's crust, and ferromanganese minerals are sensitive to changes in redox condition. The redox-sensitive dynamics and budget of ferromanganese minerals are important for understanding the global cycling of manganese and numerous associated trace elements [1]. At present, the most extensive deposition of ferromanganese minerals occurs on the deep-seafloor in oceanic abyssal plains, including those below open-ocean gyres. However, the extent of ferromanganese minerals buried in subseafloor sediments remains unclear.

During the Integrated Ocean Drilling Program (IODP) Expedition 329, we drilled the entire sedimentary sequence at six sites in the ultra-oligotrophic region of the South Pacific Gyre (SPG), where dissolved O_2 and aerobic microbial communities are present from the seafloor to the ~100 million-year-old sediment-basement interface [2]. By establishing an improved method for the observation of sediment microstructure [3], we found abundant (10^8–10^9 particles/cm^3; average, 3.34 × 10^8 particles/cm^3) micrometer-scale ferromanganese mineral particles (Mn-microparticles) (Fig. 1) in the oxic pelagic clays of the SPG [4]. Furthermore, we established a microparticle separation technique by the combined use of density concentration [5] and flow cytometer/particles sorting [6]. Major and trace element compositional analyses by inductively coupled plasma-mass spectrometry (ICP-MS) revealed that iron and manganese were the major components of Mn-microparticles, while they also contained rare-earth elements (REEs). REE concentration patterns in these Mn-microparticles reveal predominantly positive cerium anomalies.

Bulk sample X-ray absorption fine structure (XAFS) analysis indicates the manganese oxidized state. The X-ray absorption near-edge structure (XANES) spectra at the Mn K-edge [Fig. 2(a)] of the bulk sediments herein exhibited absorption maxima similar to that of MnO_2 references such as δ-MnO_2 and birnessite. The extended X-ray absorption fine structure (EXAFS) spectra of selected samples [Fig. 2(b)] also showed dominant Mn(IV) in the bulk sample studied herein. However, scanning transmission X-ray microscopy (STXM) analysis of a separated Mn-microparticle indicated the manganese reduced state. The near-edge X-ray absorption fine structure (NEXAFS) spectra of manganese at the Mn L-edge of the separated Mn-microparticle exhibited absorption patterns similar to spectra of Mn(II) reference. Thermodynamic calculations of the redox state of the SPG sediment porewater suggest that Mn(II) minerals are unsaturated, which precludes precipitation of Mn(II) minerals in the oxic subseafloor environment. We conclude that (1) the primary redox state of manganese in the Mn-microparticles is oxidized and

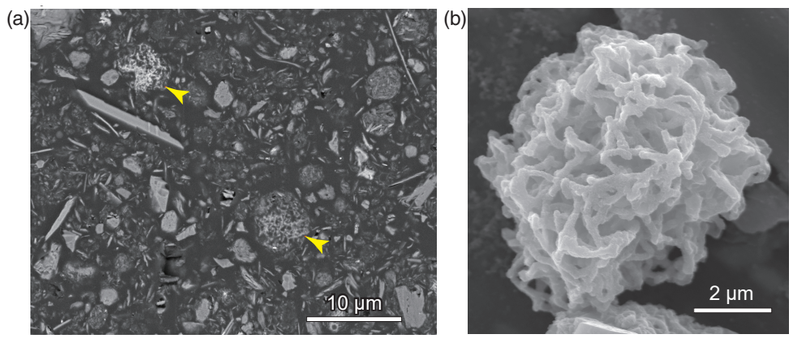

Figure 1: Representative electron micrographs of Mn-microparticles in sediment samples. (a) Cross-sectional scanning electron microscopy (SEM) images of resin-embedded oxic pelagic clay. Arrows indicate Mn-microparticles. (b) SEM image of a Mn-microparticle in a density-separated sample (sample U1365C-1H-2 0/20).

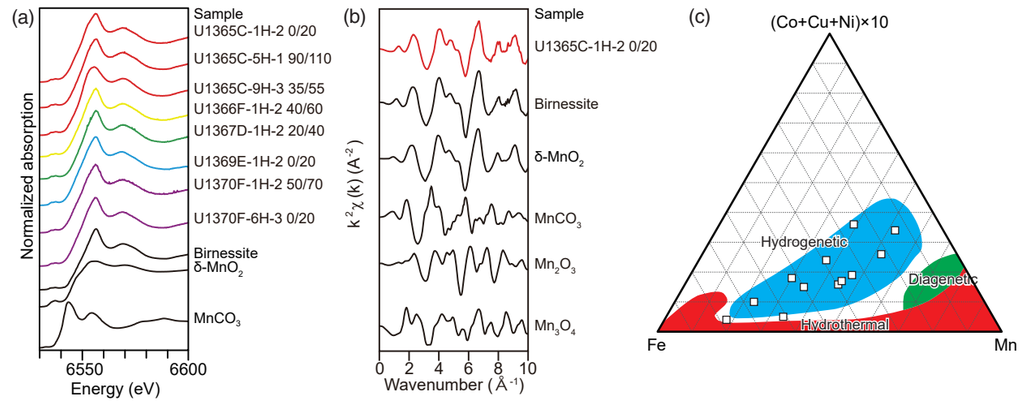

Figure 2: Geochemical characteristic of manganese in Mn-microparticles in oxic pelagic sediments. (a) XANES spectra of selected and standard samples. (b) Representative normalized k^2-weighted EXAFS spectra for sample U1365C-1H-2 0/20 and standard samples. (c) Fe-Mn-(Co + Cu + Ni)×10 ternary diagram showing the origin of Mn-microparticles.

(2) photoreduction of manganese in Mn-microparticles may have occurred via irradiation by the intense X-rays during STXM measurements. Careful adjustment of the absorbed number of photons in a unit volume of sample and X-ray exposure time enables precise determination of the manganese redox state in Mn-microparticles.

Based on the major and trace elemental composition of Mn-microparticles (such as Fe-Mn-(Co+Cu+Ni)×10 ternary diagram [7] and values of Ce anomaly) and primary redox state of manganese in sediments, we interpret that Mn-microparticles in oxic SPG sediments were formed primarily by the hydrogenetic precipitation of manganese oxides from bottom water [Fig. 2(c)]. Together with this, the distribution of Mn-microparticles even in deep and old (~100 Ma) sediment indicates that the Mn-microparticles have been stable since their deposition over ~100 Ma. Since the Mn-microparticles are thought to be stable in the sediment, we can infer the flux of Mn-microparticles into the oxic sediments from the abundance in the sediment and its sedimentation rate. The Mn-microparticles are calculated to form and precipitate at a rate of 108 ± 35 microparticles/cm^2-sediment per day.

This study based on the multidisciplinary characterization of Mn-microparticles provides a basis for understanding the global distribution and budget of manganese contained in Mn-microparticles within deep-sea oxic sediments. If we assume that the number of Mn-microparticles in the SPG pelagic clay is roughly constant at 3.34 × 10^8 cm^{-3}, and accounts for changes in manganese content in Mn-microparticles with sediment depth (>40–70% in shallow sediments and <1.8% in deep sediments) and the global distribution of oxic pelagic clay [2], an estimated 1.5–8.8 × 10^{28} Mn-microparticles are present in the oxic pelagic clays, corresponding to 1.28–7.62 Tt of manganese. Our manganese budget estimate from Mn-microparticles is at least 2–3 orders of magnitude higher than those presented in previous studies based on seafloor manganese nodules and crusts [8]. Along with the examination of manganese input, formation, and preservation, the discovery of abundant Mn-microparticles provides new insight into the global manganese budget.

REFERENCES

[1] J. E. Post, *Proc. Natl. Acad. Sci. U. S. A.* **96**, 3447 (1999).
[2] S. D'Hondt, F. Inagaki, C. A. Zarikian, L. J. Abrams, N. Dubois, T. Engelhardt, H. Evans, T. Ferdelman, B. Gribsholt, R. N. Harris, B. W. Hoppie, J.-H. Hyun, J. Kallmeyer, J. Kim, J. E. Lynch, C. C. McKinley, S. Mitsunobu, Y. Morono, R. W. Murray, R. Pockalny, J. Sauvage, T. Shimono, F. Shiraishi, D. C. Smith, C. E. Smith-Duque, A. J. Spivack, B. O. Steinsbu, Y. Suzuki, M. Szpak, L. Toffin, G. Uramoto, Y. T. Yamaguchi, G.-l. Zhang, X.-H. Zhang and W. Ziebis, *Nat. Geosci.* **8**, 299 (2015)
[3] G.-l. Uramoto, Y. Morono, K. Uematsu and F. Inagaki, *Limnol. Oceanogr. Methods* **12**, 469 (2014).
[4] G.-l. Uramoto, Y. Morono, N. Tomioka, S. Wakaki, R. Nakada, R. Wagai, K. Uesugi, A. Takeuchi, M. Hoshino, Y. Suzuki, F. Shiraishi, S. Mitsunobu, H. Suga, Y. Takeichi, Y. Takahashi and F. Inagaki, *Nat. Comm.* **10**, 400 (2019).
[5] R. Wagai, M. Kajiura, M. Asano and S. Hiradate, *Geoderma* **241**, 295 (2015).
[6] Y. Morono, T. Terada, J. Kallmeyer and F. Inagaki, *Environ. Microbiol.* **15**, 2841 (2013).
[7] E. Bonatti, T. Kraemer and H. Rydell, "Classification and Genesis of Submarine Iron-Manganese Deposits" in *Ferromanganese Deposits on the Ocean Floor,* edited by R. H. David, p.149-166 National Science Foundation, 1972.
[8] J. M. Broadus, *Science* **235**, 853 (1987).

BEAMLINES

BL-9A and BL-13A

G.-I. Uramoto[1, 2], Y. Morono[1], N. Tomioka[1], S. Wakaki[1], R. Nakada[1], R. Wagai[3], K. Uesugi[4], A. Takeuchi[4], M. Hoshino[4], Y. Suzuki[4, 5], F. Shiraishi[5], S. Mitsunobu[7], H. Suga[5], Y. Takeichi[8], Y. Takahashi[5] and F. Inagaki[1] ([1]JAMSTEC, [2]Kochi Univ., [3]NARO, [4]JASRI, [5]The Univ. of Tokyo, [6]Hiroshima Univ., [7]Ehime Univ., [8]KEK-IMSS-PF)